Characterization of the Effect of Cold Joints and Functional Grading in Stepwise Constructed Tensile Dog Bones with Embedded Digital Image Correlation

Tomislav Kosta, Claron J. Ridge, Marcel M. Hatter, and Jesus O. Mares

Abstract We present an extension of our previously published work in which we utilized an in situ/embedded Digital Image Correlation (DIC) technique to evaluate the effect of aging on the interface debonding strength in an idealized particulate composite. The idealized composite consists of a single ~650 μm glass bead inclusion at the center of a Sylgard 184 dog bone tensile sample along with an embedded DIC speckle pattern at the mid-plane. The speckle pattern enables the measurement of the strain field in the region surrounding the embedded glass bead while the sample undergoes a tensile load to failure. The measured strain field can then be used in conjunction with the global load measurement to characterize the local stress required to induce a failure at the interface. In previous works we have demonstrated how this approach can be used to characterize interface debonding. Construction of these tensile samples is done in a stepwise fashion with partial cure cycles in order to achieve a reliable in situ/embedded DIC speckle pattern. This stepwise construction introduces two uncertainties into the experiment, namely, cold joints between the casting layers and functional grading of the stiffness properties due to each layer experiencing different curing histories. In this work we present an evaluation of the effect of the cold joints and functional grading by performing tension tests to measure the global stiffness of dog bones of various sample configurations spanning the number of cold joints and the cure cycle history. By comparing the measured stiffness of each sample configuration, the effect of the cold joints and functional grading are determined.

Keywords DIC · Tension testing · Sylgard · Cold joints · Functional grading

Introduction

The bulk mechanical properties of polymer matrix composites depend highly upon the mechanical properties of the individual components as well as the interfaces between those components. This is especially true under tensile loading where weak interface adhesion can lead to interface debonding which ultimately reduces the integrity and load carrying capability of the material. In particulate composites the total interface area can be significant, especially for high volume fraction filled materials; therefore interface adhesion and strength can have a strong effect on tensile strength properties. Due to the stochastic nature of failure as well as the technical challenges involved in measuring interface debonding in particulate composites, it is difficult to achieve an accurate statistical representation of the debonding process.

Several standard methods exist to measure the adhesion of a simple binary material system; however, these tests are typically conducted to provide qualitative comparisons to indicate increased or decreased adhesion relative to a baseline. Tests such as the peel, [1], pull [2], and blister test [3] provide a means of quantifying the debonding process; however, these tests are not well suited for particulate composite materials due to sample geometry and size requirements. While it is possible to fabricate samples which would enable use of these tests, the data would not be representative due to differences in properties such as surface morphology, etc.

T. Kosta (✉) · C. J. Ridge · J. O. Mares
United States Air Force Research Laboratory, Munitions Directorate, Eglin AFB, FL, USA
e-mail: tomislav.kosta@us.af.mil; claron.ridge.1@us.af.mil; jesus.mares.2@us.af.mil

M. M. Hatter
University of Dayton Research Institute, Dayton, OH, USA
e-mail: Marcel.hatter.ctr@us.af.mil

C. Franck et al. (eds.), *Challenges in Mechanics of Biological Systems and Materials, Thermomechanics and Infrared Imaging, Time Dependent Materials and Residual Stress, Volume 2*, Conference Proceedings of the Society for Experimental Mechanics Series,
https://doi.org/10.1007/978-3-031-50470-9_14

Various approaches have been published which provide a more direct means of characterizing the interface debonding behavior and are more well suited for particulate composites. For example, Tan et al. [4] have recently integrated Digital Image Correlation (DIC) into a mode-I fracture test of a composite with a high volume fraction of particulate filler and an elastomeric matrix material to provide targeted data for calibration of a cohesive zone element (CZE) model. These experiments offer a measurement of interface debonding behavior; however, the statistical distribution of the properties of individual interfaces is partially lost due to the integrated nature of the measurement.

Alternatively, experiments such as those by Gent and Park [5] and proposed by Lauke [6, 7] explicitly consider the debonding of a single filler particle within a matrix material. The work by Gent and Park [5] examines the debonding of a single glass sphere embedded in an optically transparent matrix material. Under a tensile load, the onset of interface debonding was observed, and the local stress state was analytically determined using the load frame force measurement and sample geometry configuration. A critical debonding stress was noted to serve as an indicator of the strength of adhesion between the filler particle and the matrix material.

In previous work [8], we presented an extension of the technique proposed by Gent and Park [5], where we incorporated embedded DIC to better quantify the interface debonding event. Our approach utilizes an embedded DIC speckle pattern to quantify the strain field surrounding the mid-plane of a glass sphere embedded at the center of an optically transparent polymer material. We are able to quantitatively capture the strain field during a tensile loading event from the initial unloaded state up to and through the debonding event. Our approach is briefly summarized in the following section; however, the reader is referred to [8] for a more complete discussion.

In this work, we investigate various aspects of the sample fabrication procedure to determine the effect, if any, on the interpretation of the acquired data. Our approach necessitates a stepwise fabrication of the tensile samples which involves multiple casting and curing steps in order to ensure proper placement of the embedded glass sphere and DIC speckle pattern. An artifact of having multiple cast and cure steps is a functional grading of the elastic properties through the thickness of the tensile samples, as well as cold joints between the various casting layers.

Experimental Method

Summary of Tensile Test Technique

We briefly summarize our technique to characterize interface debonding using an embedded DIC approach here; however, the reader is referred to [8] for a more complete discussion.

Tensile test samples, or "dog bones," are constructed using a multiple-step process to create an embedded glass bead within an elastomeric material with an embedded field of tracking particles at the mid-plane. In order to achieve optical access to the glass bead of interest, a transparent matrix material of polydimethylsiloxane (PDMS) is used. The tensile test samples have a nominal gage section of 9 mm width by 12 mm thickness. We use commercially available Sylgard 184 from Dow Corning as the PDMS matrix material, a ~650 μm 3M hollow glass microsphere for the primary inclusion, and 27–32 μm Cospheric black polyethylene microspheres to construct a layer of fine tracking particles around the glass bead which serves as the DIC speckle pattern. The optical properties of all components allow for direct observation of the embedded DIC speckle pattern during the tensile test. This ensures that the calculation of the strain field surrounding the glass bead during loading and the debonding event can be achieved. A diagram of a fully constructed sample is shown in Fig. 1.

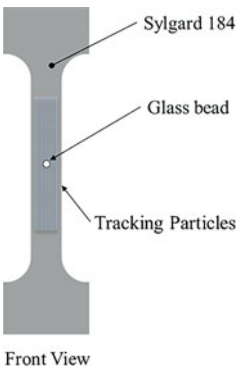

Fig. 1 Diagram of fully constructed tensile test sample with embedded DIC speckle pattern and glass bead inclusion [8]

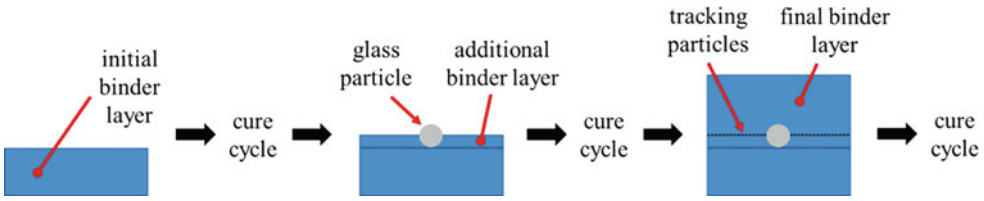

Fig. 2 Layered approach to constructing tensile test samples with embedded DIC speckle pattern and glass bead inclusion [8]

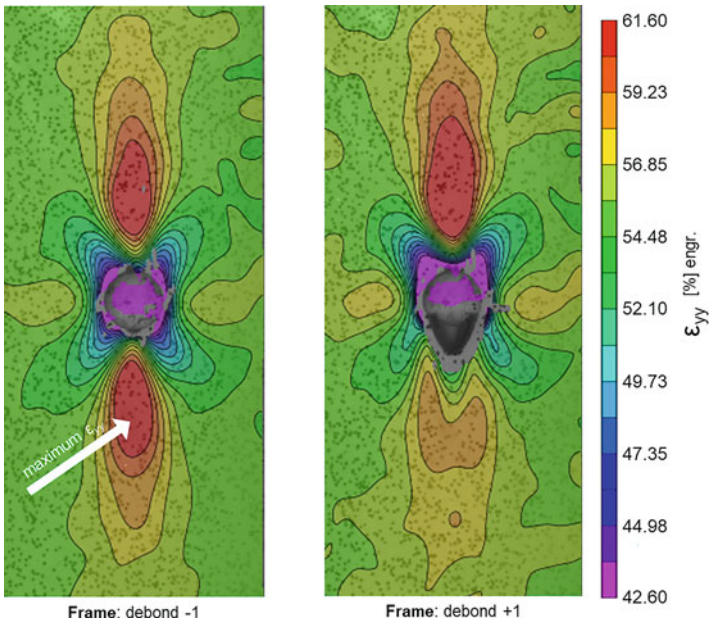

Fig. 3 The location of the maximum local tensile strain is indicated. Example of calculated strain field in the vicinity of the embedded particle in the vertical direction one frame pre-debond and one frame post-debond [8]

Construction of the samples is completed in a stepwise fashion with multiple casting and curing steps. This multiple step fabrication process enables placement of the glass bead at the approximate center of the dog bone and the DIC speckle pattern at the approximate mid-plane of the sample and bead. First, a base layer of matrix material is poured into the mold and then partially cured at 70 °C for 30 min to provide a solid base to place the glass bead upon. Second, a thin layer of matrix material is added to the partially cured base layer, the glass bead is placed, and the entire assembly undergoes a second cure cycle at 70 °C for 30 min. Third, the fine tracking particles are deposited on the cured surface of the second layer, and the remaining thickness of the mold is filled with matrix material. The entire sample assembly undergoes a third and final cure cycle at 70 °C for 30 min. The entire fabrication process is depicted in Fig. 2.

After fabrication, samples are stored under ambient conditions in the laboratory for a period of at least 3 weeks before testing. This time period is based on the results of an aging study we conducted recently [9] in which we found that the elastic modulus of Sylgard 184 continues to increase after fabrication for approximately 3–4 weeks and then reaches an asymptotic value. After the allotted time, each sample is tested using a conventional load frame. A tensile load is applied at 0.5 mm/s in order to apply a constant engineering strain rate. The evolution of the speckle pattern is captured by a 4 MP camera which is mounted on a translating stage to ensure the region of interest remains in the field of view of the camera due to the highly compliant nature of the elastomer matrix.

The resulting data includes a stress vs. strain curve from the load frame and a time series of images from the camera. The stress-strain curve provides the global stress in the gage section of the dog bone. The speckle pattern images are processed in a commercial DIC application to obtain the time-resolved two-dimensional strain field surrounding the glass bead inclusion from the unloaded state up to and through the debonding event. Figure 3 shows the calculated strain field in the vertical direction one frame pre-debond and one frame post-debond. The combination of the global stress measurement and the local strain field provides a rich data set describing the debonding process.

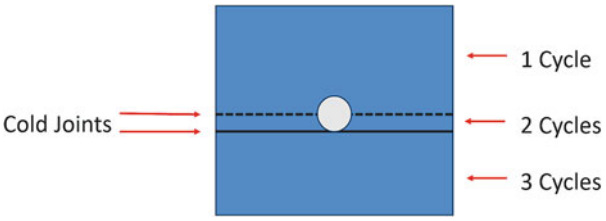

Fig. 4 Cross-section diagram of tensile dog bone sample highlighting the cold joints and functionally graded layers

Functional Grading and Cold Joints

While our fabrication approach is necessary for placement of the embedded glass bead and DIC speckle pattern, the presence of functional grading and cold joints caused by this process is unrepresentative of a homogeneous matrix material. Due to the multi-step casting and curing process, the base layer is exposed to three cure cycles, while the top layer is exposed to only one cure cycle. A fully constructed tensile sample consisted of three layers and two cold joints: the base layer, middle layer, and top layer with one cold joint between the base/middle layers and one cold joint between the middle/top layers, as depicted in Fig. 4.

Each cure cycle is prescribed at 70 °C for 30 min using a convection oven, with each casting step taking approximately 10 min. For reference, Dow specifies various cure times for Sylgard 184 ranging from 48 h at 25 °C to 10 min at 150 °C [10]. While each cure cycle is the same temperature and time duration, it follows that the base layer is cured for a total of 90 min, the middle layer is cured for a total of 60 min, and the top layer is cured for a total of 30 min. A natural consequence of this is that for a freshly fabricated fully constructed sample, each layer may have different mechanical properties. It is important to quantify this functional grading as it may have implications on data interpretation and computational model calibration. It is also important to quantify the effect of the presence of the cold joints for the same reasons.

To evaluate the effect of the functional grading and cold joints, we have devised two series of experiments to compare the effective bulk mechanical properties of homogeneous and multiple step constructed samples. The first series aims to specifically evaluate the functional grading, and the second series evaluates the presence of the cold joints. In both series, sample testing was conducted approximately 3 weeks after sample fabrication in accordance with the recommendations in our Sylgard 184 aging study to allow for the natural aging to stabilize [9].

For the functional grading study, three sets of six samples were produced. Each sample was cast to a “full” sample thickness of approximately 12 mm in a single casting step. Each set was then cured in a convection oven at 70 °C for 30, 60, and 90 min, respectively. The samples which were cured for 60 and 90 min were allowed to remain in the oven for the full duration rather than being pulled from the oven as they would be for a typical sample fabrication process. Each dog bone was individually packaged and stored in the same laboratory as the tensile load frame. All sample fabrication and testing were completed by the same operator using the same oven and load frame. Two different molds were used to expedite the fabrication process; however, both molds are nominally the same geometry. Tensile testing was completed using an MTS Exceed E42.503 5 kN load frame with a 1 kN load cell. All samples were aged for a prescribed 27 days.

For the cold joint study, three sets of 12 samples were produced. Each batch of dog bone samples was cast with one, two, or three layers to represent each stage of sample production. The first set was cast as a single layer of full 12 mm thickness with a single cure cycle for 30 min at 70 °C. The second set was fabricated in two steps, each 6 mm thickness, and two 30-min cure cycles at 70 °C. The third set was fabricated in three steps with each layer having the same thickness as a typical fully constructed sample and cured in three 30-min cycles at 70 °C. The first sample set of this series is essentially the same as the 30-min cure sample set of the functional grading series. Each dog bone sample was individually packaged and stored in the same laboratory as the tensile load frame. As with the functional grading series, all sample fabrication and testing were completed by the same operator using the same oven and load frame. Each set was fabricated using two available molds, with both molds having the same nominal geometry. Tensile testing was completed after samples were aged between 21 and 24 days using an MTS Exceed E42.503 5 kN load frame with a 1 kN load cell.

Results

For the functional grading study, batches of six samples were fabricated at three separate curing conditions for a total of 18 samples. Each batch was cured at 30, 60, and 90 min, respectively, at 70 °C and represents each of the three layers of a fully

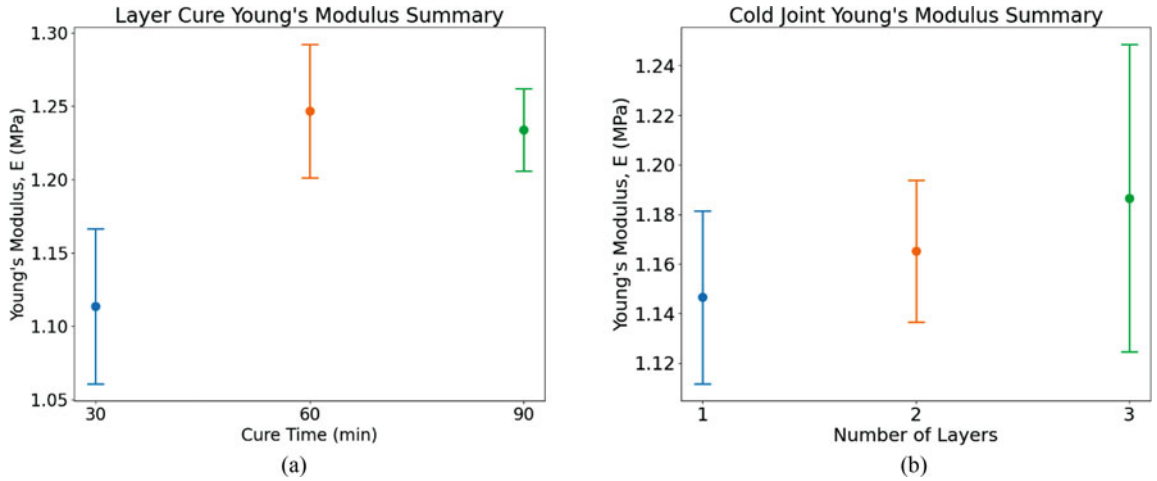

Fig. 5 Summary of results for functional grading study (**a**) and cold joint study (**b**)

constructed tensile sample (see right-most cross section of Figs. 2 and 4). The metric of interest from each tensile test was chosen as the slope of the stress-strain curve up to 25% strain. This slope represents the Young's modulus of the material and was determined using linear regression. The Young's modulus for the 30-, 60-, and 90-min cure samples was measured to be 1.114 ± 0.053 MPa, 1.247 ± 0.046 MPa, and 1.234 ± 0.028 MPa, respectively, where the values reported are the arithmetic mean and one standard deviation. These data are plotted in Fig. 5a. It is observed that the mean Young's modulus for the 60- and 90-min cure time samples is within one standard deviation between these batches, indicating no significant difference between the stiffness of the materials. However, it is observed that the mean Young's modulus of the 30-min cure time samples is 11.4% lower than the mean of the 60- and 90-min mean Young's modulus values. Additionally, the mean value of the 30-min cure time sample is outside of the standard deviation of the other two longer cured samples and indicates a more compliant material.

For the cold joint study, batches of 12 samples were fabricated for three separate layering conditions to produce a total of 36 samples. The first sample batch consisted of a single layer (no cold joints), the second sample set consisted of two layers (one cold joint), and the third sample set consisted of three layers (two cold joints). The metric of interest from each tensile test was again chosen as the slope of the stress-strain curve up to 25% strain to represent the Young's modulus of the material and was determined using linear regression. The Young's modulus for the single-, two-, and three-layer sample sets were measured to be 1.147 ± 0.035 MPa, 1.165 ± 0.029 MPa, and 1.187 ± 0.062, respectively, where the values reported are the arithmetic mean and one standard deviation. These data are plotted in Fig. 5b. It is observed that the mean of the moduli of the single- and double-layer samples lies within one standard deviation of the "full" three-layer samples. Furthermore, the difference of the mean Young's modulus between the three-layer system and the single homogeneous system is 0.04 MPa. These results indicate that there is no significant difference in the stiffness between the layered systems.

Conclusion

In this work we have built upon our previously developed technique [8] in order to further understand the capability and limitations of our approach. We have investigated the effect of functional grading and cold joints due to the sample fabrication process on the bulk elastic stiffness of our tensile test samples. We have conducted two test series to investigate these two effects and have concluded that there is no significant difference in the Young's modulus across each of the three layers. Additionally, we conclude that there is no significant influence of the cold joints on the bulk stiffness of our tensile samples. For further data processing, modeling, and simulation efforts, the stepwise constructed tensile dog bone samples can be considered as a simplified monolithic sample with minimal effects due to the functional grading and cold joints.

Acknowledgments The authors would like to thank the Air Force Office of Scientific Research for funding this work under grant 20RWCOR094. This work is Distribution A: Approved for public release, distribution unlimited (AFRL-2013-0813).

References

1. ASTM D1876-08(2015)e1: Standard Test Method for Peel Resistance of Adhesives (T-Peel Test). ASTM International, West Conshohocken (2015)
2. ASTM D4541-17: Standard Test Method for Pull-Off Strength of Coatings Using Portable Adhesion Testers. ASTM International, West Conshohocken (2017)
3. ASTM D6900-10(2015): Standard Test Method for Wet Adhesion of Latex Paints to a Gloss Alkyd Enamel Substrate. ASTM International, West Conshohocken (2015)
4. Tan, H., Liu, C., Huang, Y., Geubelle, P.H.: The cohesive law for the particle/matrix interfaces in high explosives. J. Mech. Phys. Solids. **53**(8), 1892–1917 (2005)
5. Gent, A., Park, B.: Failure processes in elastomers at or near a rigid spherical inclusion. J. Mater. Sci. **19**(6), 1947–1956 (1984)
6. Lauke, B.: Determination of adhesion strength between a coated particle and polymer matrix. Compos. Sci. Technol. **66**(16), 3153–3160 (2006)
7. Lauke, B.: Stress field calculation around a particle in elastic–plastic polymer matrix under multiaxial loading as basis for the determination of adhesion strength. Compos. Interf. **23**(1), 1–14 (2016)
8. Kosta, T., Mares, J.O.: Characterization of interface debonding behavior utilizing an embedded digital image correlation scheme. In: Lin, M.T., Furlong, C., Hwang, C.H. (eds.) Advancement of Optical Methods & Digital Image Correlation in Experimental Mechanics. Conference Proceedings of the Society for Experimental Mechanics Series. Springer, Cham (2021). https://doi.org/10.1007/978-3-030-59773-3_11
9. Kosta, T., Mares Jr., J.O., Hatter, M.M., Resue, B.M., Ridge, C.J.: The effect of aging on delamination strength utilizing an embedded digital image correlation scheme. In: Amirkhizi, A., Furmanski, J., Franck, C., Kasza, K., Forster, A., Estrada, J. (eds.) Challenges in Mechanics of Time-Dependent Materials & Mechanics of Biological Systems and Materials, Volume 2. SEM 2022. Conference Proceedings of the Society for Experimental Mechanics Series. Springer, Cham (2023). https://doi.org/10.1007/978-3-031-17457-5_13
10. "SYLGARD™ 184 Silicone Elastomer Technical Data Sheet." [Online]. Available: https://www.dow.com/content/dam/dcc/documents/en-us/productdatasheet/11/11-31/11-3184-sylgard-184-elastomer.pdf